Proceedings of the 17th World Congress
The International Federation of Automatic Control
Seoul, Korea, July 6-11, 2008

Multivariable LQG Control of a Proton Exchange Membrane Fuel Cell System

Fu-Cheng Wang*, Hsuan-Tsung Chen, Jia-Yush Yen

Mechanical Engineering Department, National Taiwan University, Taipei 10617, Taiwan
*(*Tel:+886233662680, e-mail:fcw@ntu.edu.tw, d89522001@ntu.edu.tw, jyen@ntu.edu.tw)*

Abstract: This paper applies multivariable linear quadratic Gaussian (LQG) control strategies to a proton exchange membrane fuel cell (PEMFC) system. From the system point of view, a PEMFC can be modeled as a two-input-two-output system, where the inputs are air and hydrogen flow rates and the outputs are cell voltage and current. By fixing the output resistance, we aimed to control the cell voltage output by regulating the air and hydrogen flow rates. Due to the nonlinear characteristics of this system, multivariable LQG controllers were designed to provide steady voltage output and to reduce the hydrogen consumption of this system. The study was carried out in three parts. Firstly, the PEMFC system was modelled as multivariable transfer function matrices using identification techniques. Secondly, LQG control algorithms were utilized to design a multivariable controller. Finally, the designed controller was implemented to control the air and hydrogen flow rates. From the experimental results, multivariable LQG control is deemed effective in providing steady output responses and significantly reducing hydrogen consumption.

1. INTRODUCTION

Alternative energy resources have drawn much attention in recent years due to the decrease in fossil fuel deposit and deterioration of greenhouse effect. Among them, the proton exchange membrane fuel cell (PEMFC) is a crucial candidate for replacing traditional fuel because of its favourable characteristics, including low operation temperature, fast power response, high power density, low noise pollution, high system efficiency and environmental friendliness. Recently, PEMFC has been applied to many systems such as vehicles, boats, etc. (Chen and Peng, 2005, Jay, Peng and Stefanopoulou, 2004). In such systems, batteries and DC/DC converters were used to provide steady output voltage. However, the use of those peripheral components may degrade the efficiency of the fuel cell system. In addition, most system utilized traditional control methodologies such as process control to operate the PEMFC. Nevertheless, these control methods cannot provide good system performance and may even cause instability due to the nonlinear characteristics of the fuel cell system. Therefore, in this paper we consider the closed-loop structures of the PEMFC system, and apply LQG control strategies to improve system stability and performance.

(Forrai et al., 2005) applied system identification methods to model a PEMFC system as a circuit consisting of inner resistors and a capacitor. (Woo and Benziger, 2007) designed a proportional-integral-derivative (PID) controller to regulate the hydrogen flow rate and tuned the oxygen flow at a ratio of 1.3:2 (O_2:H_2) to obtain optimal performance. (Vega-Leal et al., 2007) developed a multi-input-single-output (MISO) system to control the output current. They designed a feed-forward controller to adjust the air flow rate, and a proportional controller to regulate temperature so that the net power is optimized. (Methekar,Prasad and Gudi, 2007) considered a multi-input-multi-output (MIMO) system with inputs of hydrogen and coolant and outputs of power density and temperature, and proposed two PID control strategies. Many studies have utilized hybrid systems to improve overall system performance. (Thounthong, Rael and Davat, 2006) integrated a fuel cell and super-capacitors for electric vehicles. They aimed to control the transient power through PID control of the super-capacitors, while the fuel cell operated at a steady rate. For some applications, the DC/DC converters were utilized to increase system efficiency. (Wai, Liu and Duan, 2006) employed the voltage-clamped and soft-switching techniques to design a DC/DC converter. (Zenith and Skogestad, 2007) utilized sliding mode control to adjust the duty cycle of a rapid DC/DC converter to control the output voltage.

Because a steady power source is important for electrical equipment, (Wang et al., 2006, Wang et al., 2007b) applied H_∞ robust control to a single-input-single-output (SISO) PEMFC system to achieve steady voltage output by regulating the oxygen flow rate. The experimental results illustrated that robust controllers can cope with system perturbations and achieve splendid performance. Furthermore, the robust control can also replace the DC/DC converter and broaden the applications. The ideas were extended in (Wang et al., 2007a) to a multi-input PEMFC system, in which the proposed multivariable robust controllers can provide steady voltage and reduce hydrogen consumption by regulating the air and the hydrogen flow rates simultaneously. In this paper, we applied LQG control to the PEMFC system. The work is arranged as follows: in Section 2 fuel-cell dynamics is described and modelled as a MIMO system. In Section 3, LQG control strategies are introduced and apply to design a controller for the system. In Section 4, PWM theory is introduced and applied to control the hydrogen valve of the PEMFC system. In Section 5, the designed controller is implemented to verify their performance. Finally, we draw some conclusions in Section 6.

2. IDENTIFICATION OF THE FUEL CELL SYSTEM

In this section, fuel cell dynamics is described and modelled as a MISO system, for which identification techniques are applied to obtain the system transfer functions. Those transfer functions will then be used for the controller design in Section 3.

2.1 System Description

The fuel-cell system considered in this paper was designed and manufactured by CSIST (Chung Shan Institute of Science and Technology) and integrated by DELTA Electronics™. The inputs of the system are hydrogen and air while the outputs are cell voltage and current. The system consists of 15 cells with an active area of 50 cm^2 on each. The maximum efficiency of the fuel cell stack is 37% (Lower Heating Value, LHV) under dry H_2/air and humidification-free conditions (Wang et al., 2007b).

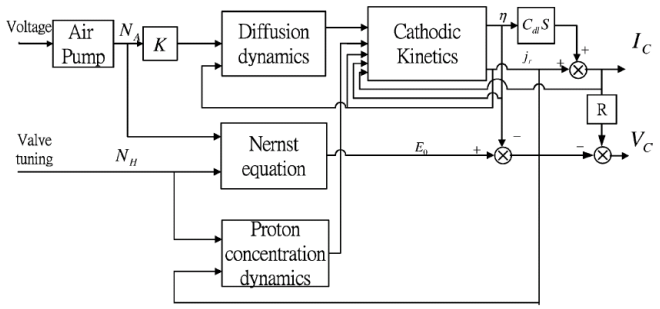

Fig. 1.The dynamics of the PEMFC.

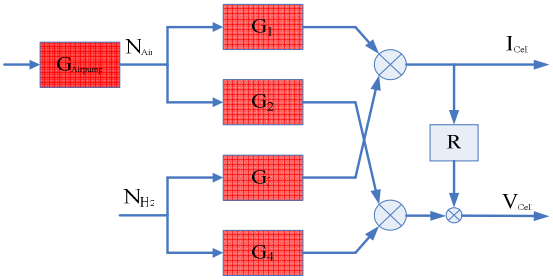

Fig. 2.The block diagram of the fuel cell system.

The dynamics of the fuel-cell system is non-linear and time-varying in that it is influenced by many factors, including the diffusion dynamic, the Nernst equation, proton concentration dynamics and cathode kinetics (Ceraolo, Miulli and Pozio, 2003), as shown in Fig. 1. Nevertheless, from the system point of view, the fuel-cell dynamics can be represented as a MIMO system, as depicted in Fig. 2, with the following relation (Maciejowski and Chang, 1991):

$$I_{cell} = G_1 N_{Air} + G_3 N_{H_2} \quad (1)$$

$$V_{cell} = G_2 N_{Air} + G_4 N_{H_2} - R \cdot I_{cell} \quad (2)$$

in which G_1~ G_4 represent the input-output relationship of the system. It is noted that the dynamics of the linearized model depends on the operating conditions. For example, when the current load varies from 2A to 6A, the output voltage decreases significantly from 11V to 7.5V using the on-board controller, as illustrated in Fig. 3. Therefore, we apply LQG control algorithms to obtain steady outputs even when the operating conditions change. By fixing the output resistance, we can either control the cell voltage or current output by tuning the air (N_{air}) and hydrogen (N_{H_2}) flow rates. Since most electrical equipment requires constant voltage supply, in this paper we aim to control the cell voltage output.

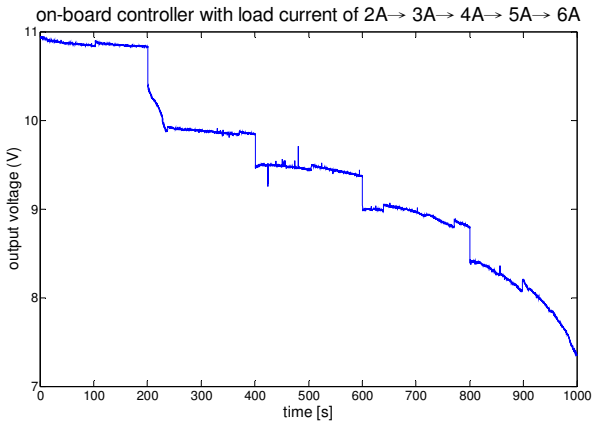

Fig. 3.Voltage variations with changing current loads.

2.2 System identification

In order to describe the transfer functions of (1, 2), we measured the input and output signals of the fuel cell system, and utilized subspace system identification methods to estimate the models in state-space form, as presented in the following (Goethals et al., 2005):

$$\begin{cases} x_{t+1} = Ax_t + Bu_t + w_t \\ y_t = Cx_t + v_t \end{cases}, \quad (3)$$

in which $u_t \in \mathbb{R}^m$ and $y_t \in \mathbb{R}^l$ are the input and output signals, while $x_t \in \mathbb{R}^n$ represents the state and $w_t \in \mathbb{R}^n$, $v_t \in \mathbb{R}^l$ are zero mean white Gaussian noise vector sequences.

For the experiments, a chirp signal and a pseudo-random binary signal (PRBS) were generated to control the air pump and the hydrogen valve of the PEMFC system, respectively, as shown in Fig. 4. Both the frequencies of the chirp signal and PRBS were set at 0.01~5Hz (see Fig. 5 (a)). We set the current loadings as 2A, 3A and 4A, and measured the output voltage responses, as illustrated in Fig. 5 (b). In order to take system variation into account, we repeated the experiments three times at each operating condition, and employed the aforementioned identification techniques to obtain the corresponding transfer functions, as illustrated in Table 1. Those transfer functions will be utilized for LQG controller design in Section 3.

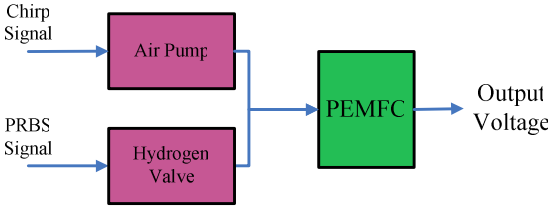

Fig. 4.The MISO blocks structure of the PEMFC system.

	2A	3A	4A
1	$G_{11}=\begin{bmatrix}\frac{0.00202z-0.001598}{z^2-1.954z+0.9555} & \frac{0.000505z-0.0003996}{z^2-1.954z+0.9555}\end{bmatrix}$	$G_{21}=\begin{bmatrix}\frac{0.001935z-0.00153}{z^2-1.971z+0.973} & \frac{0.0004837z-0.0003824}{z^2-1.971z+0.973}\end{bmatrix}$	$G_{31}=\begin{bmatrix}\frac{0.001603z-0.001052}{z^2-1.934z+0.9373} & \frac{0.0004z-0.0002629}{z^2-1.934z+0.9373}\end{bmatrix}$
2	$G_{12}=\begin{bmatrix}\frac{0.00156z-0.001158}{z^2-1.976z+0.9771} & \frac{0.0003901z-0.0002896}{z^2-1.976z+0.9771}\end{bmatrix}$	$G_{22}=\begin{bmatrix}\frac{0.001919z-0.001483}{z^2-1.974z+0.9753} & \frac{0.0004798z-0.0003708}{z^2-1.974z+0.9753}\end{bmatrix}$	$G_{32}=\begin{bmatrix}\frac{0.001774z-0.001231}{z^2-1.932z+0.9354} & \frac{0.0004435z-0.0003077}{z^2-1.932z+0.9354}\end{bmatrix}$
3	$G_{13}=\begin{bmatrix}\frac{0.0006934z-0.000162}{z^2-1.942z+0.9457} & \frac{0.0001733z-0.0000405}{z^2-1.942z+0.9457}\end{bmatrix}$	$G_{23}=\begin{bmatrix}\frac{0.00154z-0.000985}{z^2-1.948z+0.95} & \frac{0.0003851z-0.0002462}{z^2-1.948z+0.95}\end{bmatrix}$	$G_{33}=\begin{bmatrix}\frac{0.001483z-0.0009106}{z^2-1.918z+0.9208} & \frac{0.0003707z-0.0002277}{z^2-1.918z+0.9208}\end{bmatrix}$

Table 1. Transfer functions at the operation points.

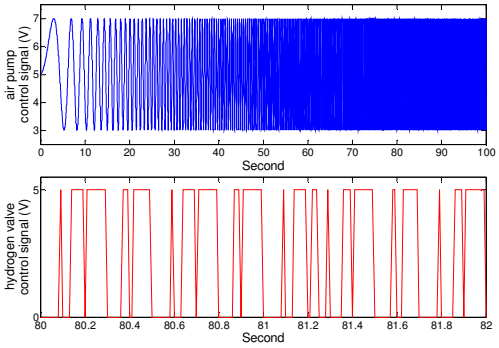

(a) The input signals.

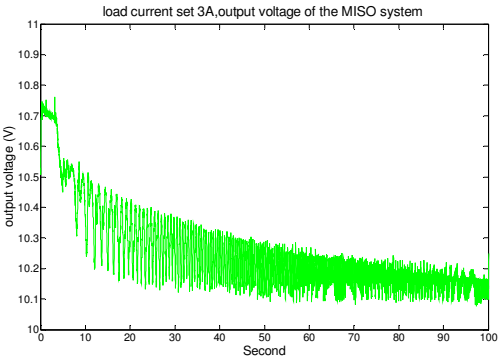

(b) The output voltage responses.

Fig. 5 The input and output signals of the system.

2.3 Selection of the nominal plant

For the LQG controller design, the nominal plant is selected to minimize the size (in terms of gap metric) of plant perturbations. The *gap metric* between two systems G_0 and G_Δ can be defined as follow (Georgiou and Smith, 1990):

> *The smallest value of* $\|[\Delta_M, \Delta_N]\|_\infty$ *which perturbs* G_0 *into* G_Δ, *is called the gap between* G_0 *and* G_Δ, *and is denoted as* $\delta(G_0, G_\Delta)$.

The selection of the nominal plants $G_0(s)$ was based on the calculation of gaps between the nominal plants and the perturbed plants, such that the maximum gap is minimized as:

$$\min_{G_0} \max_{G_i} \delta(G_0, G_\Delta). \tag{4}$$

Considering the system transfer function matrices in Table 1 (sampling time: 0.01 second), the gaps between all plants are illustrated in Table 2. Therefore, G_{23} was selected as the nominal plants for the MISO system because the maximum gap between it and other plants is 0.2449, which is the minimum of all systems.

Table 2. Gaps of the plants.

	G_{11}	G_{12}	G_{13}	G_{21}	G_{22}	G_{23}	G_{31}	G_{32}	G_{33}
G_{11}	0	0.2127	0.1346	0.1278	0.3054	0.0751	0.078	0.0966	0.0956
G_{12}	0.213	0	0.3395	0.2098	0.2137	0.1649	0.2858	0.3034	0.3044
G_{13}	0.135	0.3395	0	0.2068	0.4254	0.1932	0.0585	0.039	0.0488
G_{21}	0.128	0.2098	0.2068	0	0.3522	0.1327	0.161	0.1785	0.1922
G_{22}	0.305	0.2137	0.4254	0.3522	0	0.2449	0.3736	0.3902	0.3844
G_{23}	0.075	0.1649	0.1932	0.1327	0.2449	0	0.1366	0.1551	0.1522
G_{31}	0.078	0.2858	0.0585	0.161	0.3736	0.1366	0	0.0195	0.0341
G_{32}	0.097	0.3034	0.039	0.1785	0.3902	0.1551	0.0195	0	0.0263
G_{33}	0.096	0.3044	0.0488	0.1922	0.3844	0.1522	0.0341	0.0263	0
Max	0.305	0.3395	0.4254	0.3522	0.4254	0.2449	0.3736	0.3902	0.3844

3. LQG CONTROLLER DESIGN

In this section, the LQG control algorithms are introduced. Using the selected nominal plant, we design a LQG controller to stabilize the fuel cell system and to achieve the optimal performance.

3.1. LOG Control Algorithms (Skogestad, 1996):

The name LQG arises from the use of a linear model, an integral Quadratic cost function, and Gaussian white noise processes to model disturbances and noises. Consider a state-space mode as follows:

$$\begin{aligned} \dot{x} &= Ax + Bu + w_d \\ y &= Cx + v_n \end{aligned}, \tag{5}$$

where w_d and v_n are the disturbance and measurement noise inputs respectively, which are usually assumed to be uncorrelated zero-mean Gaussian stochastic processes with constant power spectral density. The LQG control problem is to find the optimal control $u(t)$ which minimizes cost function J_r:

$$J_r = \int_0^\infty \left(x(t)^T Qx(t) + u(t)^T Ru(t) \right) dt \,, \tag{6}$$

where the weighting matrices Q and R are used to define the compromise between regulation performance and control effort. The LQG design follows the well known Separation Principle, which consists of the optimal state estimator and the optimal state feedback designs, as shown in Fig. 6. Firstly, for the optimal state feedback control problem, we consider a linear quadratic regulator (LQR) program, which can be regarded as a simplified problem without w_d and v_n. The solution is as follows:

$$u(t) = -K_r x(t) \,, \tag{7}$$

where $K_r = R^{-1}B^T X$ and $X = X^T \geq 0$ is the unique positive-semi-definite solution of the following algebraic Riccati equation:

$$A^T X + XA - XBR^{-1}B^T X + Q = 0 \,. \tag{8}$$

The next step is to find the optimal estimation of state x, denoted as $\hat{x}$, so that $E((x-\hat{x})(x-\hat{x})^T)$ is minimized. The Kalman filter utilizes the following state estimator:

$$\dot{\hat{x}} = A\hat{x} + Bu + K_f (y - C\hat{x}) \,, \tag{9}$$

in which the optimal choice of K_f is given by

$$K_f = YC^T V^{-1} \,, \tag{10}$$

where $Y = Y^T \geq 0$ is the unique positive-semi-definite solution of the following algebraic Riccati equation:

$$YA^T + AY - YC^T V^{-1} CY + W = 0 \,. \tag{11}$$

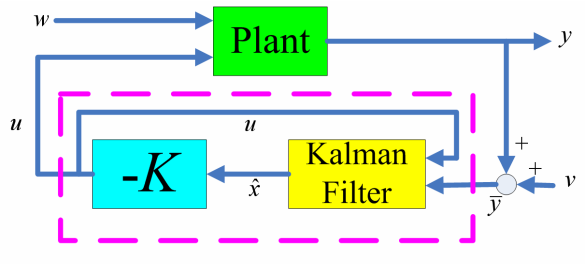

Fig. 6. LQG regular structure.

Therefore, the solution to the LQG problem is formed by replacing x with $\hat{x}$, and denoted by $u(t) = -K_r \hat{x}(t)$. Finally, the transfer function of the LQG regulator can be written as

$$K_{LQG}(s) = \begin{bmatrix} A - BK_r - K_f C & K_f \\ -K_r & 0 \end{bmatrix} = \begin{bmatrix} A - BR^{-1}B^T X - YC^T V^{-1} C & YC^T V^{-1} \\ -R^{-1}B^T X & 0 \end{bmatrix} , \tag{12}$$

To eliminate the steady state error, a weighting function W was applied in the controller design, as shown in Fig. **7**.

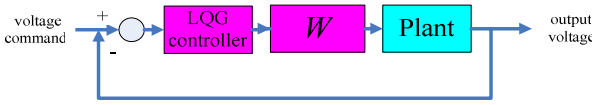

Fig. 7. LQG tracking structure.

However, for the LQG design, the system stability cannot be guaranteed unless R in (6) tends to zero, which is known as the Loop Transfer Recovery (LTR) procedure. In practice, the resulting controller is difficult to implement in that the process ($R \to 0$) may result in high gains and cause problems in the presence of un-modelled dynamics. Therefore, R is not usually taken to the limits of 0 to achieve full recovery. In stead, a set of designs is obtained using small *R's*. Then an acceptable design is selected. From the experiments, we set R=0.1 in this paper to adjust the feedback gain.

4. PULSE WIDTH MODULATION THEORY

To control the hydrogen valve, we utilized the Pulse Width Modulation (PWM) theory. In recent years, the combination of PWM and fast-switch valves has been widely applied in many control fields, such as position control of pneumatic actuators (Topcu,Yuksel and Kamis, 2006). PWM is a modulation technique which utilizes a carry function to generate variable-width pulses, in order to represent the amplitude of an input signal. As illustrated in Fig. 8, given the input signal and carry function, a comparator is applied to compare the magnitudes of these two signals to generate the modulated signal. When the input signal is greater than the carry signal, the modulated signal is set to be "high". Otherwise, it is set to be "low". In Fig. 8 (b), the period of the modulated signal is the same as the period of the carry signal, T_c. Furthermore, the duty ratio τ of the modulated signal is defined as:

$$\tau = T_{on} / T_c \tag{13}$$

in which T_{on} is the operating time. In our applications, more hydrogen is supplied when τ is increased. To regulate the hydrogen flow, we employed a 2/2-way MAC 35A-AAA-DAA-1BA valve with a switch frequency of about 1kHz and a maximum power consumption of 5.4 W (MAC-VALVES). For the MISO experiments, we applied a carry function with a frequency of 10 Hz and maximum amplitude of 1V to control the hydrogen valve. The resulting MISO controller was then combined with PWM theory and experimentally applied to verify the effect.

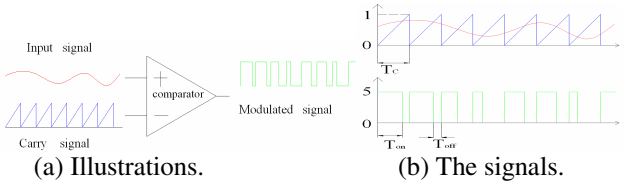

(a) Illustrations. (b) The signals.

Fig. 8. Working principle of Pulse Width Modulation.

5. EXPERIMENTAL RESULTS

In order to implement the designed controller, we employed Matlab with a DAQ card to control the PEMFC system. The control structure in Matlab/Simulink is illustrated in Fig. 9.

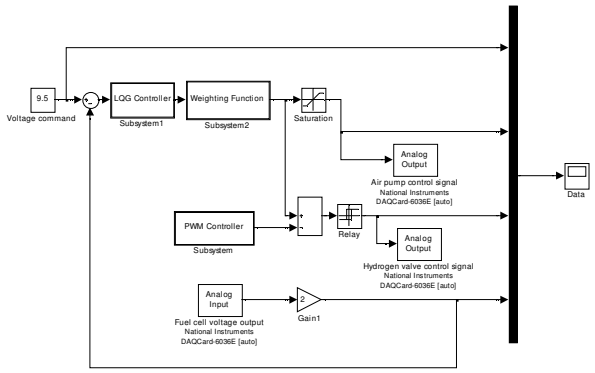

Fig. 9. The control structure in Matlab/Simulink.

For the MISO system,

$$G_{23}=\begin{bmatrix}\dfrac{0.00154z-0.000985}{z^2-1.948z+0.95} & \dfrac{0.0003851z-0.0002462}{z^2-1.948z+0.95}\end{bmatrix} \quad (14)$$

was selected as the nominal plant (sampling time: 0.01 second). Setting R= 0.1 and the following weighting function:

$$W=\begin{bmatrix}\dfrac{z-0.99}{z-1} & 0\\ 0 & \dfrac{0.008}{z-1}\end{bmatrix}, \quad (15)$$

the corresponding controller was designed as follow:

$$K_{23}(z)=\begin{bmatrix}\dfrac{0.5384z^2-1.0507z+0.5128}{z^3-2.7821z^2+2.5885z-0.8032}\\ \dfrac{0.0286z^2-0.056z+0.0274}{z^3-2.7821z^2+2.5885z-0.8032}\end{bmatrix}, \quad (16)$$

We implemented $K_{23}(z)$ (sampling time: 0.01 second) and set the reference voltage as 9.5v, the experimental results are shown in Fig. 10, with the fixed current settings of 2A, 3A and 4A in (a), (b) and (c), respectively, and a varied current loading of 2A→3A→4A in (d). The corresponding output voltage and hydrogen consumption are compared with the SISO study in (Wang et al., 2007b). Firstly, it is noted that both the multivariable LQG controller and the SISO robust controller stabilized the system and achieved similar voltage responses. On the other hand, the hydrogen consumption was significantly reduced by the multivariable LQG controller. For quantitative comparison, Table 3 illustrates the RMS error of the output voltage and the average duty ratio of the hydrogen valve calculated from Fig. 10. It is noted that the hydrogen consumption was reduced to about 20-30%, as compared to the SISO controller (Wang et al., 2007b) (for which the hydrogen flow was fixed at 1.2 LPM, and by air flow was controlled to provide steady cell voltage). That is, the hydrogen consumption was regulated according to the current loads to avoid waste of fuel. To conclude, the MISO designed controller has not only achieved steady voltage output, but also exhibits reduced hydrogen consumption.

Table 3. Statistic data from Fig. 10(with settings of 9.5v)

		2A (a) 20s →300s	3A (b) 20s →300s	4A (c) 20s →300s	2A→3A→4A (d)		
					20s →100s	100s →200s	200s →300s
MISO LQG control	RMS error	0.0389	0.0314	0.0237	0.009	0.0255	0.0203
	Average air pump voltage (V)	2.5994	2.7854	3.1356	2.5362	2.7899	3.0084
	Average hydrogen flow rate (LPM)	0.24	0.2818	0.3582	0.24	0.2772	0.3582
SISO H_∞ control	RMS error	0.023	0.038	0.033	0.029	0.063	0.049
	Average air pump voltage (V)	2.06	3.425	3.2	2.33	2.74	3.78
	Average hydrogen flow rate (LPM)	1.2	1.2	1.2	1.2	1.2	1.2

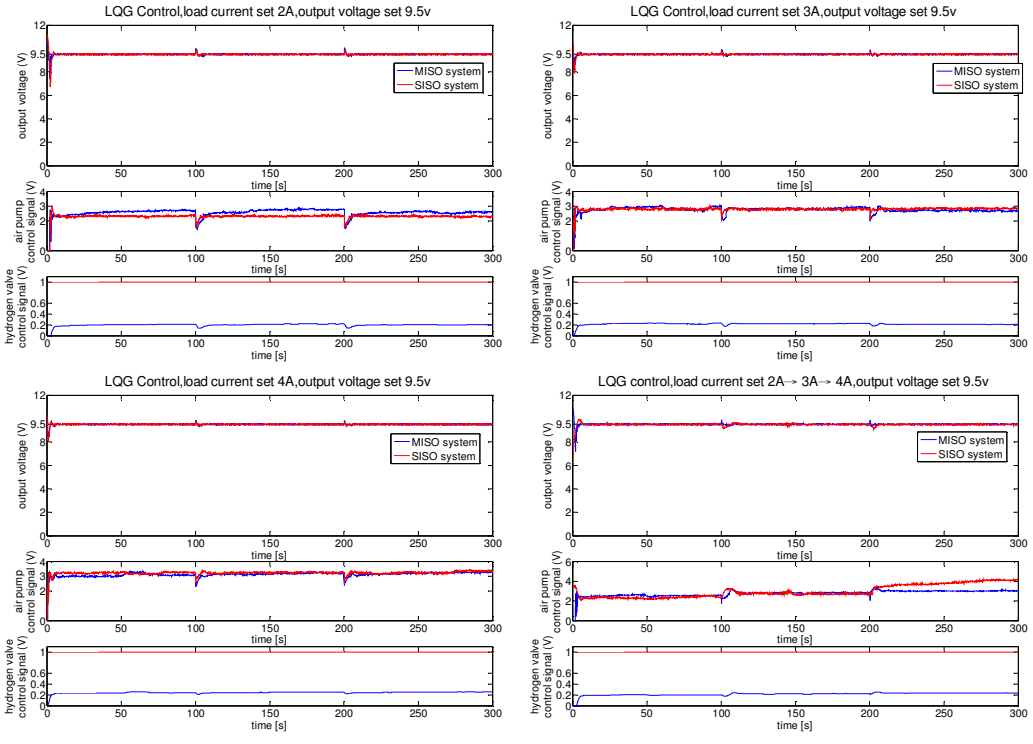

Fig. 10. The comparison of voltage responses and hydrogen consumption using SISO and MISO controllers.

In Fig. 11, we set the voltage command as 7.5V→8.5V→9.5V→8.5V→7.5V, with current loads of 3A and 4A. Firstly, the controller demonstrated excellent tracking ability with the voltage command. Furthermore, Tables 4 illustrates the statistical data calculated from Fig. 11. It is noted that the hydrogen consumption was significantly reduced from 1.2 LPM (liter per minute) to about 0.24-0.36 LPM. And the system consumed more hydrogen when the power load was increased.

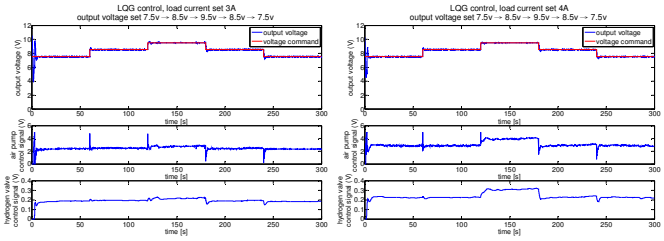

(a) 3A load. (b) 4A load.

Fig. 11. The voltage responses and control signals, with settings of 7.5v→8.5v→9.5v→8.5v→7.5v.

Table 4. Statistic data from Fig. 11

MISO		7.5v 20s →60s	8.5v 60s →120s	9.5v 120s →180s	8.5v 180s →240s	7.5v 240s →300s
RMS error	3A	0.01	0.056	0.0644	0.0785	0.0672
	4A	0.0173	0.0542	0.0569	0.095	0.0749
Average air pump voltage (V)	3A	2.3974	2.4725	2.7498	2.4017	2.3258
	4A	2.8558	2.8643	3.9305	2.8917	2.8466
Average hydrogen flow rate (LPM)	3A	0.24	0.24	0.2582	0.24	0.24
	4A	0.3159	0.3418	0.36	0.3298	0.3336

6. CONCLUDING REMARKS

In this paper, a multivariable LQG controller has been designed and implemented on a PEMFC system. At first, the dynamics of the PEMFC was described and modelled as a MIMO system. By fixing the output resistance, we have succeeded in controlling the output voltage by regulating the hydrogen and air flow rates through the designed multivariable controller. The experimental results showed that using a suitable weighting function, the proposed multivariable LQG controller not only provided steady voltage output even when the operating conditions change, but also significantly reduced the hydrogen consumption of the PEMFC system.

ACKNOWLEDGEMENT

The authors would like to thank Delta Electronics™ for providing the portable PEMFC system studied in this paper.

REFERENCE

Ceraolo, M., C. Miulli and A. Pozio (2003) Modelling static and dynamic behaviour of proton exchange membrane fuel cells on the basis of electro-chemical description. *Journal of Power Sources,* **113,** 131-144.

Chen, D. and H. Peng (2005) A Thermodynamic Model of Membrane Humidifiers for PEM Fuel Cell Humidification Control. *Journal of Dynamic Systems, Measurement, and Control,* **127,** 424-432.

Forrai, A., et al. (2005) Fuel-Cell Parameter Estimation and Diagnostics. *Energy Conversion, IEEE Transaction on,* **20,** 668-675.

Georgiou, T. T. and M. C. Smith (1990) Optimal robustness in the gap metric. *Automatic Control, IEEE Transactions on,* **35,** 673-686.

Goethals, I., et al. (2005) Subspace identification of Hammerstein systems using least squares support vector machines. *Automatic Control, IEEE Transactions on,* **50,** 1509-1519.

Jay, T. P., H. Peng and A. G. Stefanopoulou (2004) Control-Oriented Modeling and Analysis for Automotive Fuel Cell Systems. *Journal of Dynamic Systems, Measurement, and Control,* **126,** 14-25.

MAC-VALVES *http://www.macvalves.com/home.html*.

Maciejowski, J. M. and B. C. Chang (1991) Multivariable feedback design. *Applied Mechanics Reviews,* **44,** 114.

Methekar, R. N., V. Prasad and R. D. Gudi (2007) Dynamic analysis and linear control strategies for proton exchange membrane fuel cell using a distributed parameter model. *Journal of Power Sources,* **165,** 152-170.

Skogestad, S. (1996) Multivariable feedback control : analysis and design. Wiley. New York

Thounthong, P., S. Rael and B. Davat (2006) Control strategy of fuel cell/supercapacitors hybrid power sources for electric vehicle. *Journal of Power Sources,* **158,** 806-814.

Topcu, E. E., I. Yuksel and Z. Kamis (2006) Development of electro-pneumatic fast switching valve and investigation of its characteristics. *Mechatronics,* **16,** 365-378.

Vega-Leal, A. P., et al. (2007) Design of control systems for portable PEM fuel cells. *Journal of Power Sources,* **169,** 194-197.

Wai, R. J., L. W. Liu and R. Y. Duan (2006) High-Efficiency Voltage-Clamped DC--DC Converter With Reduced Reverse-Recovery Current and Switch-Voltage Stress. *Industrial Electronics, IEEE Transactions on,* **53,** 272-280.

Wang, F. C., et al. (2006) Proton exchange membrane fuel cell system identification and control - Part II: H-infinity based robust control. *Proceedings of 4th International ASME Conference on Fuel Cell Science, Engineering and Technology.*

Wang, F. C., et al. (2007a) Multivariable System Identification and Robust Control of a Proton Exchange Membrane Fuel Cell System. *46th IEEE Conference on Decision and Control*

Wang, F. C., et al. (2007b) System identification and robust control of a portable proton exchange membrane full-cell system. *Journal of Power Sources,* **164,** 704-712.

Woo, C. H. and J. B. Benziger (2007) PEM fuel cell current regulation by fuel feed control. *Chemical Engineering Science,* **62,** 957-968.

Zenith, F. and S. Skogestad (2007) Control of fuel cell power output. *Journal of Process Control,* **17,** 333-347.